Complex Impedance Investigation of Epitaxial LCMO Thin Films

E. Mateev*, T. Nurgaliev and B. Blagoev

Institute of Electronics, Bulgarian Academy of Sciences, 72 Tzarigradsko Chaussee Blvd., 1784 Sofia, Bulgaria

Epitaxial $La_{0.67}Ca_{.33}MnO_3$ (LCMO) thin films by off-axis magnetron sputtering were deposited on $SrTiO_3$ (STO) substrates. Complex impedance measurements (module and phase of the thin film impedance) in frequency range 1–30 kHz are done. Substantial dependence of both: module and phase of the complex surface impedance is observed. The temperature interval scanned is from 77 K to room temperature. The impedance has inductive behavior for temperatures less than the Curie temperature and capacitive for higher temperatures. Reduction of the film thickness from 60 to 30 nm shifts the impedance curves to the lower temperatures.

1. Introduction

The perovskite manganites are an object of experimental and theoretical studies due to several reasons [1]. Colossal magnetoresistance applications [2, 3], bolometric purposes, applications as a cathode material in solid-oxide fuel cells [4].

Typical usage of the perovskite magnitoresistive materials is based on DC measurements. However, the same measurements can be done in the ac (above 1 kHz) range. The ac measurements can be more efficient, because the $1/f$ noise is strongly reduced. This makes the investigation of the ac complex resistance interesting for the applications. In the same time they give a valuable knowledge on the individual contribution of grains and grain boundaries to the low field magnetoresistance [5, 6].

In [7] are presented the results of the complex impedance frequency dependence investigation in ac range (1–100 kHz) for mono- and polycrystal LCMO layers at room temperature (under the Curie temperature). Here we present the results of the complex impedance frequency dependence investigation in the region 1–30 kHz for LCMO monocrystal layers in a temperature interval from 77 K to room temperature (the Curie temperature for LCMO is within this interval).

2. Experimental

The investigated layers were deposited on 5×10 mm^2 STO substrates by HF magnetron sputtering. The deposition temperature was 780°C and an oxidation step in 900 hPa O_2 at 500°C succeeded the deposition. In X-ray photoelectron spectroscopy (XPS) investigation of a film, deposited with the same technology is presented. It shows a good crystal quality of the film.

---

*corresponding author; e-mail: emateev@abv.bg

The scheme of the four point measurement of the thin film's complex impedance is shown in Fig. 1. An ac voltage generator is converted to ac current generator by means of a 1 MΩ resistor R. The current is approximately U_0/R, where U_0 is the ac voltage generated by the generator. The complex thin film's impedance of the layer is equal to kRU/U_0, is the complex value of the voltage drop between the 2nd and 3rd point in the 4 point set, measured by lock-in amplifier operating in differential mode. The form-factor k depends on the geometry of the 4 point set and in our case $k \approx 3$.
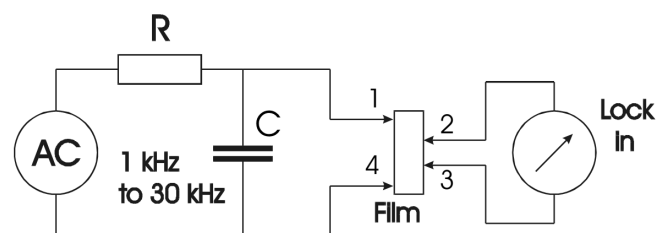

Fig. 1. Scheme of the four point measurement of the film's complex surface impedance.

In reality the situation is complicated by the fact that the resistance between the 1st and 4th points in the 4 point set can exceed 100 kΩ in the vicinity of the Curie temperature and reduce the current below U_0/R. Another factor to be taken into account is the parasitic capacitance of the wiring C. As a result it can be calculated that the current i, flowing through the film from point 1 to the point 2 of the four point structure is

$$i = \frac{U_0 - (1 + \mathrm{j}\omega RC)kU}{R + r + \mathrm{j}\omega RrC},$$

where U_0 is the ac generator's voltage, U is the voltage measured between the points 2 and 3, r is the sum of the contact resistances at points 1 and 4, k is a formfactor (ratio between the surface resistance points 1–4 to points 2–3) — in our case $k \approx 3$. The complex

surface impedance is U/I (our formfactor is ≈ 1), and neglecting r compared to R we have

$$\rho = \frac{UR}{U_0 - kU - \mathrm{j}\omega RCkU}.$$

The correction procedure has been verified by measuring two dummy objects at room temperature, each made from three equal resistors.

Two different thicknesses of the film were investigated: 30 and 60 nm. The measurements were conducted in a temperature interval from 77 K to 300 K, and frequencies from 1 kHz to 30 kHz.

3. Results and discussion

The temperature dependence of the complex thin film impedance of 30 nm LCMO layer, deposited on STO substrate, for 5 different frequencies is shown in Fig. 2a and b. The modules are shown in Fig. 2a and the phases — in Fig. 2b. The modules show a maximum, corresponding to the approximately Curie temperature. The Curie temperature of the 30 nm epitaxial layer appears substantially less than the Curie temperature of the bulk material.
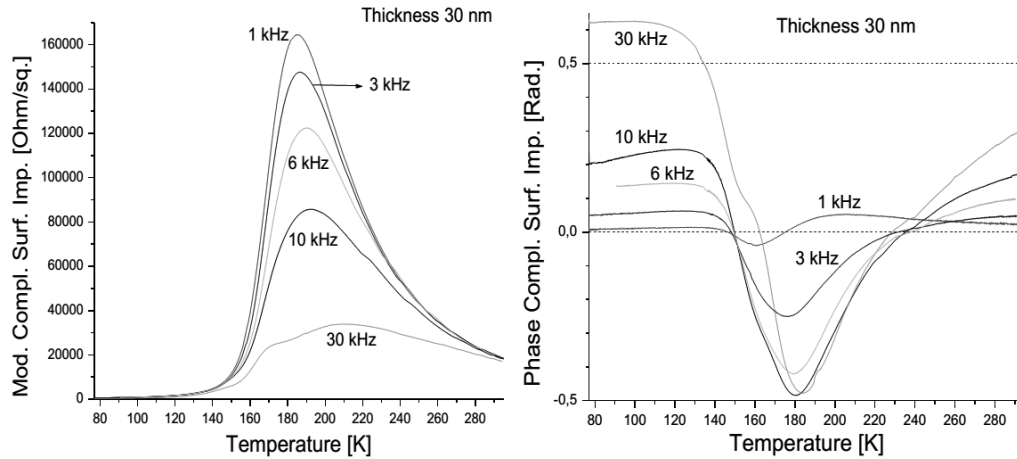

Fig. 2.   (a, left) Modules of the thin film's impedance, (b, right) phases of the thin film's impedance.
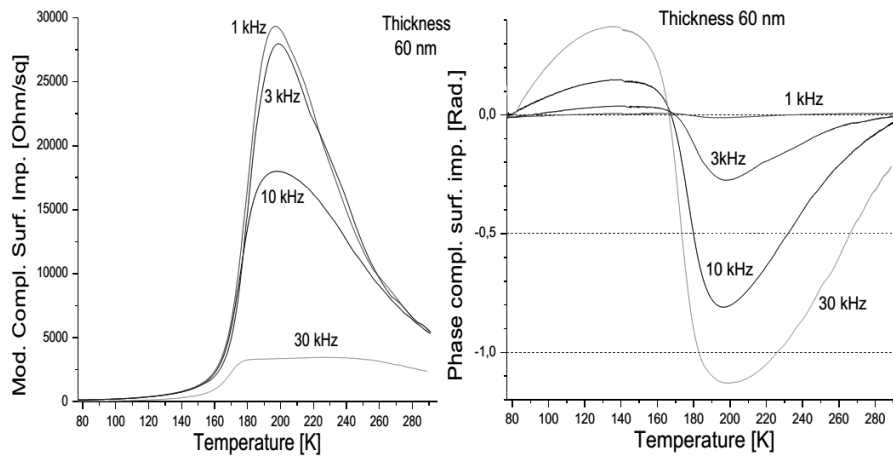

Fig. 3.   (a, left) Modules of the thin film's impedance, (b, right) phases of the thin film's impedance.

The exact values of temperature of the peaks and their values (in kΩ/sq) are shown in Table. The value of the impedance decreases with the frequency. The phase of the complex impedance is positive (inductive type) for low temperatures. This corresponds to our previously reported results of similar measurements with LCMO

surface impedance measurements at room temperature — below the Curie temperature for LCMO [7]. It goes through zero at some temperature, becomes negative (capacitive type), and has a maximum at some temperature, higher than the temperature of the module maximum. The results of a measurement at 300 Hz are not shown:

TABLE

The exact positions of the characteristic points of the curves, shown in Fig. 2a, 2b, 3a, 3b.

	1 kHz	3 kHz	6 kHz	10 kHz	30 kHz
max. module thick. 30 nm	164.5	147.6	122.5	85.7	33.9
temp. [K]	185	186.5	190	194	211
max. module thick. 60 nm	29.4	27.95		18	3.5
temp. [K]	196.5	198		197.5	227
max. pos. phase thick. 30 nm	0.015	0.06	0.15	0.25	0.62
max. pos. phase thick. 60 nm	0.008	0.038		0.15	0.37
temp. [K]	143	142		140	136
temp. of zero phase — 30 nm	146	147.5	149.4	149.6	164.6
temp. of zero phase — 60 nm	177	170		167.5	166
max. neg. phase thick. 30 nm	0.04	0.25	0.42	0.48	0.47
temp. [K]	161	176	179.5	180.5	184.5
max. neg. phase thick. 60 nm	0.011	0.275		0.804	1.13
temp. [K]	194	197.5		196.5	199

the modules curve coincides with the curve for 1 kHz, and the phase is zero (within the error limit). The exact temperatures and complex impedance values for the characteristic points are shown in Table. The temperature of the maximum impedance module is higher than the temperatures of complex impedance values characteristic points.

A capacitive nature of the impedance, observed in experiments, partly can be caused by temperature dependent permittivity of the STO substrate, where the LCMO film has been grown up. The effective dielectric constant of STO increases from ≈ 300 to ≈ 2500 when temperature is reduced from ≈ 300 K to ≈ 70 K [9–11]. For this reason it is possible a forming of capacitive connections (through high permittivity STO component) not only between the adjacent grains of LCMO layer, but between different macroareas of LCMO layer as well. This leads to a strong increase of the contribution of the capacitive component to the summary impedance at temperatures, where the resistivity of the LCMO layer and the permittivity of the STO substrate are great (especially, at the Curie temperature of the sample) (Fig. 2a and b).

The temperature dependence of the complex thin film's impedance of 60 nm LCMO layer is shown in Fig. 3a and b. The modules are shown in Fig. 3a and the phases — in Fig. 3b. The exact temperatures and complex impedance values for the characteristic points are shown in Table. The modules of impedance of the 30 nm layer is much more than twice larger than the impedance of the 60 nm layer. The phase shows differences, too. The thin layer has inductive impedance even at 77 K,

while the thick layer starts with zero and has well expressed positive impedance phase maximum at higher temperatures — see Table. All characteristic temperatures in impedance temperature dependences are higher for 60 nm layer. The maximum negative phase is twice higher for the 60 nm layer.

4. Conclusion

The complex impedance of the epitaxial LCMO layers shows substantial frequency dependence even for relatively low frequencies — 1 to 30 kHz. This cannot be explained by the common models for FM conductivity, which are dc theories.

The modules of impedance of the 30 nm layer larger than the impedance of the 60 nm layer. The phase shows differences, too. The thin layer has inductive impedance even at 77 K, while the thick layer starts with zero and has well expressed positive impedance phase maximum at higher temperatures. All characteristic temperatures in impedance temperature dependences are higher for the thicker layer. The maximum negative phase is twice higher for the 60 nm layer. All these features show that the structure of thin layers becomes different from the structure of the thick layers (bulk material). A possible explanation is that when the layer thickness becomes close to or less than the ferromagnetic domains' size their structure can change. It should be noted also that not only the structural characteristics of the substrates, but their physical (electrical) properties can affect the electrical characteristics of the films grown on them.

References

[1] V. Strbik, M. Spankova, M. Reifers, J. Kovac, S. Benacka, *J. Phys., Conf. Series* **223**, 012027 (2010).

[2] E.L. Nagaev, *Usp. Phys. Nauk* **166**, 92 (1996).

[3] S.Y. Yang, W.L. Kuang, Y. Liou, W.S. Tse, S.F. Lee, Y.D. Yao, *J. Magn. Magn. Mater.* **268**, 326 (2004).

[4] H. Rahmouni, M. Nouiri, R. Jemai, N. Kallel, F. Rzigua, *J. Magn. Magn. Mater.* **316**, 23 (2007).

[5] I.-B. Shim, K.-T. Park, C.-S. Kim, Y.-J. Oh, *J. Magn. Magn. Mater.* **226-230**, 733 (2001).

[6] H.M. Lee, I.-B. Shim, C.S. Kim, *J. Magn. Magn. Mater.* **282**, 291 (2004).

[7] E. Mateev, B. Blagoev, T. Nurgaliev, *J. Phys. Conf. Ser.* **356**, 012022 (2012).

[8] B.S. Blagoev, I.G. Gostev, T.K. Nurgaliev, V. Strbik, I.E. Bineva, L. Uspenskaya, E.S. Mateev, L. Neshkov, E. Dobročka, Š. Chromik, *Conf. Series* **514**, 012041 (2014).

[9] H.E. Weaver, *J. Phys. Chem. Solids* **11**, 274 (1959).

[10] Ch. Ang, Z. Yu, L.E. Cross, R. Guo, A.S. Bhalla, *Appl. Phys. Lett.* **79**, 818 (2001).

[11] D. Fuchs, C.W. Schneider, R. Schneider, H. Rietschel, *J. Appl. Phys.* **85**, 7362 (1999).